Understanding Collisionless Shocks in the Heliosphere

J. R. Jokipii
University of Arizona

Acknowledgements to my Arizona
Colleagues, Joe Giacalone and Jozsef Kóta .

Presented at the 5th Korean Astrophysics Workshop
"Shock Waves, Turbulence and Particle Acceleration,
Pohang, South Korea, November 18-21, 2009

Outline of Talk

- General Overview
  - Various heliospheric shocks.
  - Planar shock in a uniform medium: paradigm.
  - Energetic particles and shocks.
- Effects of Pre-existing Large-Scale Turbulence
  - Inner heliosphere.
  - Heliospheric Termination shock.

- Shocks are ubiquitous in the collisionless plasmas of space.

- shocks transfer large amounts of energy from directed plasma flows to the thermal and superthermal particle distributions.

- the plasmas are collisionless; processes at the shocks not only heat the plasma, but also result in a significant fraction (as much as ~10-20%) of the fluid flow energy being put into energetic particles, some with very high energies.

- The resulting energetic particles are ubiquitous in space, and are a significant hazard to the exploration of space. They have other important effects on the Earth's environment in space.

Shocks in the heliosphere

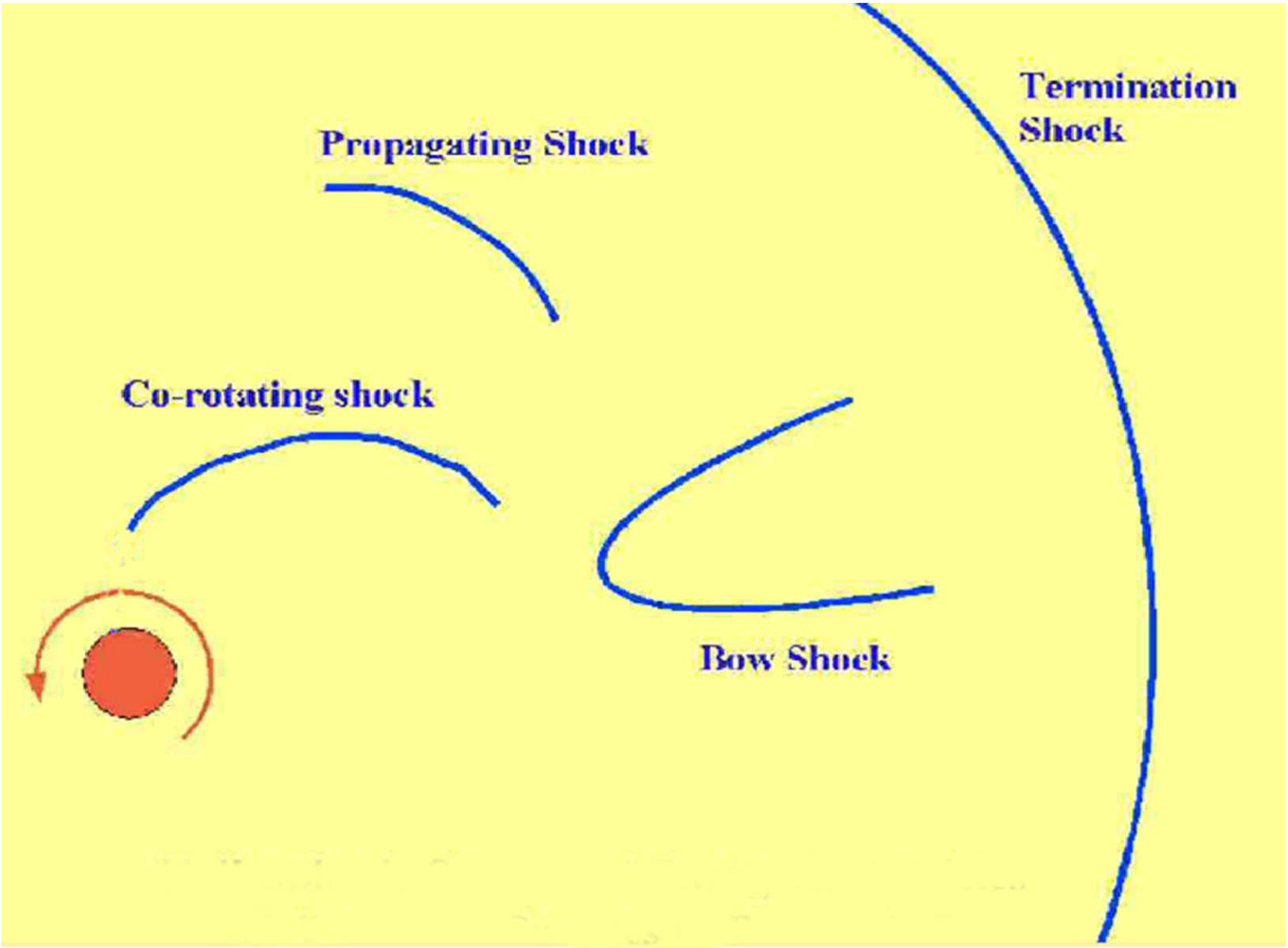

A typical propagating shock observed in the solar wind.

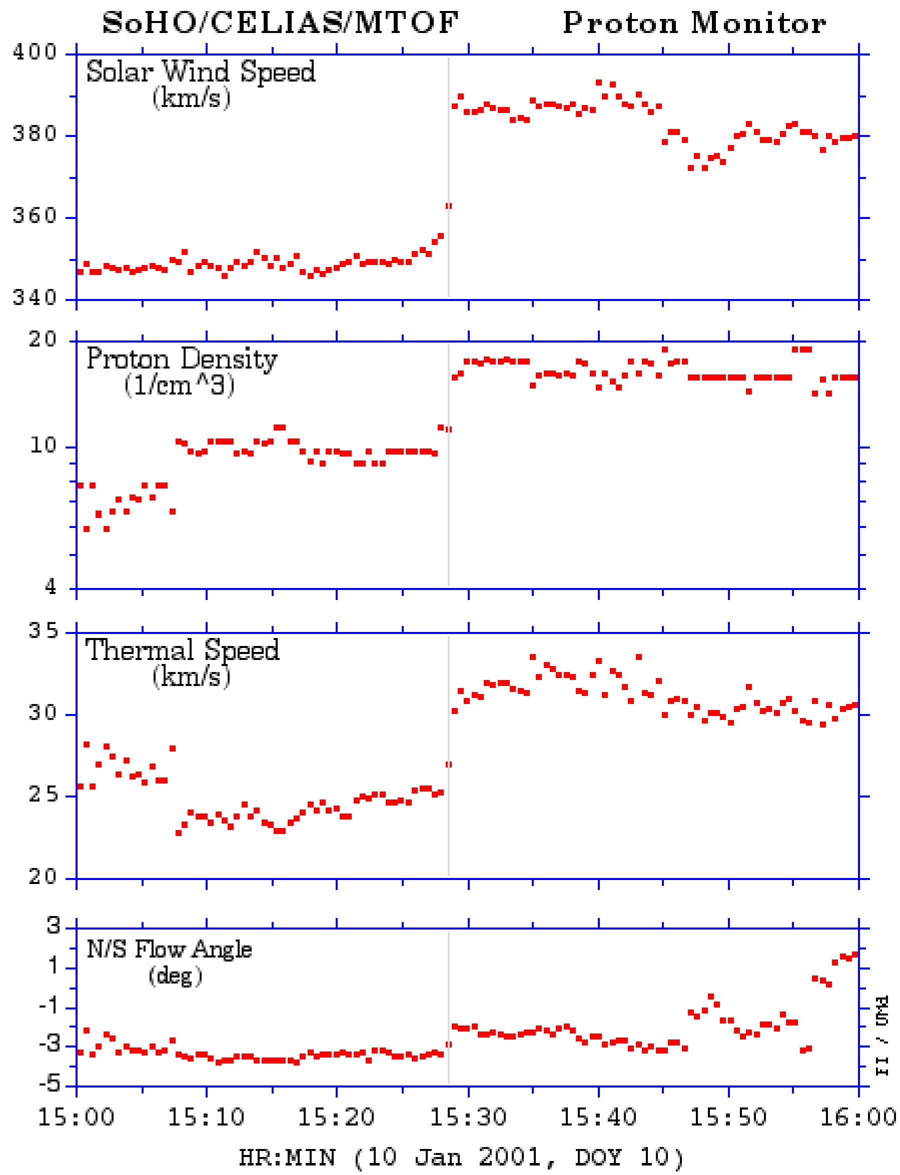

Energetic Particles

- Collisionless shocks always produce energetic particles. These are generally isotropic in pitch angle.

- The spectrum produced is generally a power law up to a time-dependent or geometry related cutoff.

- The power law produced is in a narrow range ("universal"), as is observed.

- Energetic particles are often well-described by the Parker equation since they are nearly always observed to be nearly isotropic.

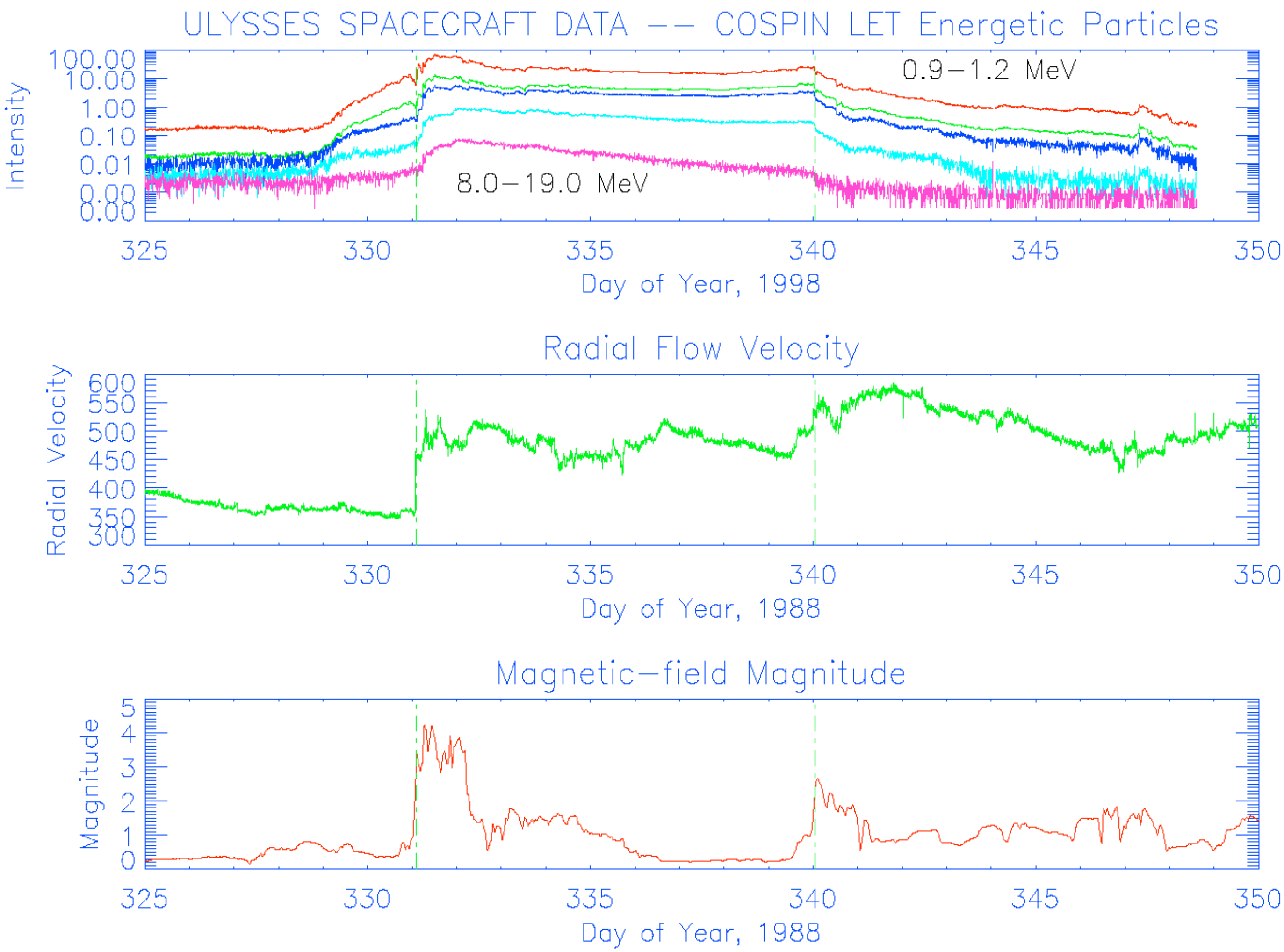
ULYSSES SPACECRAFT DATA -- COSPIN LET Energetic Particles
Intensity
100.00
10.00
1.00
0.10
0.01
0.00
0.00
0.9–1.2 MeV
8.0–19.0 MeV
325
330
335
340
345
350
Day of Year, 1998
Radial Flow Velocity
Radial Velocity
600
550
500
450
400
350
300
325
330
335
340
345
350
Day of Year, 1988
Magnetic–field Magnitude
Magnitude
5
4
3
2
1
0
325
330
335
340
345
350
Day of Year, 1988

Co-rotating interaction regions form shocks.

Co-rotating Interaction Regions

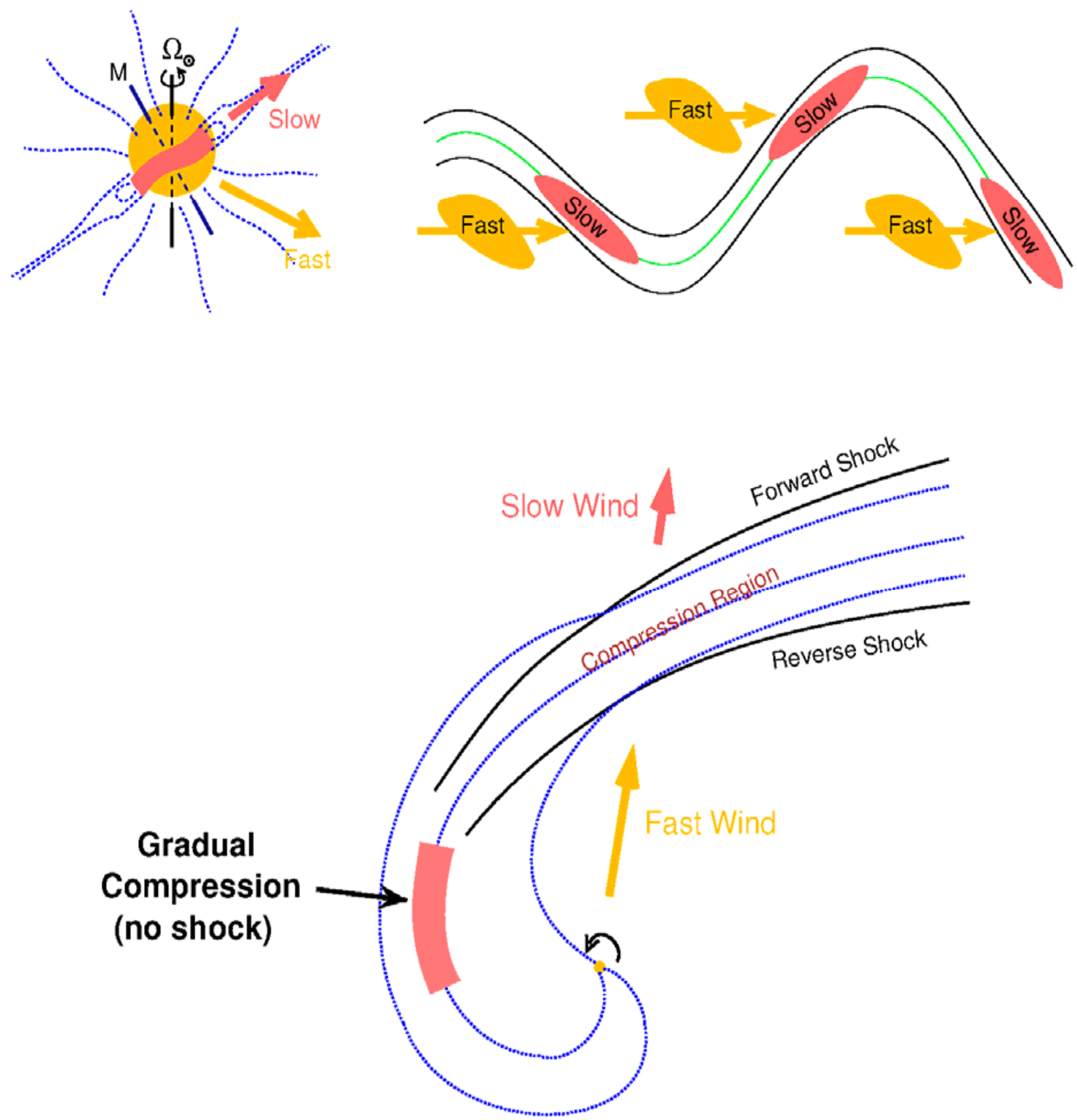

Co-rotating particle events.

Ulysses data

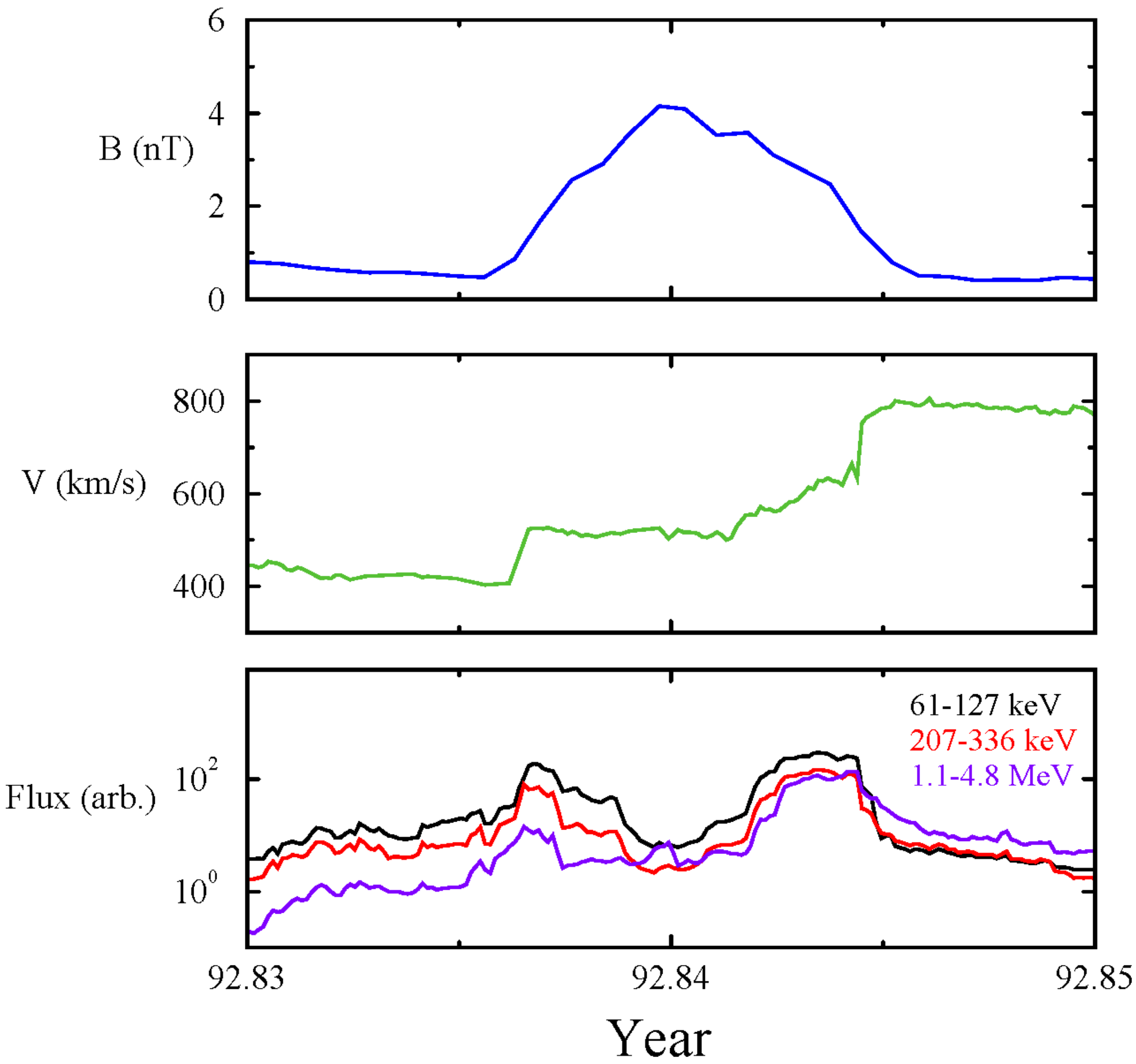

Compression of the magnetic field within CIR.

Slow, intermediate, and fast wind and both a Forward (F) and Reverse (R) shock.

Energetic Particles peaking at The F/R shocks, with a larger intensity at the <u>reverse</u> shock.

The observed energy spectra of cosmic rays are remarkably similar everywhere they are observed.

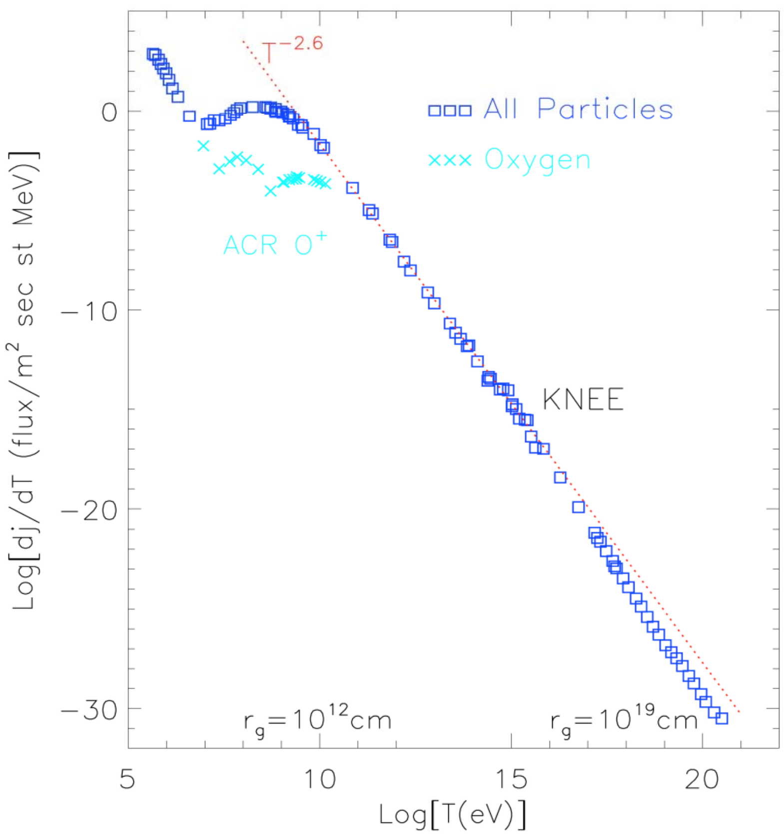

The Galaxy

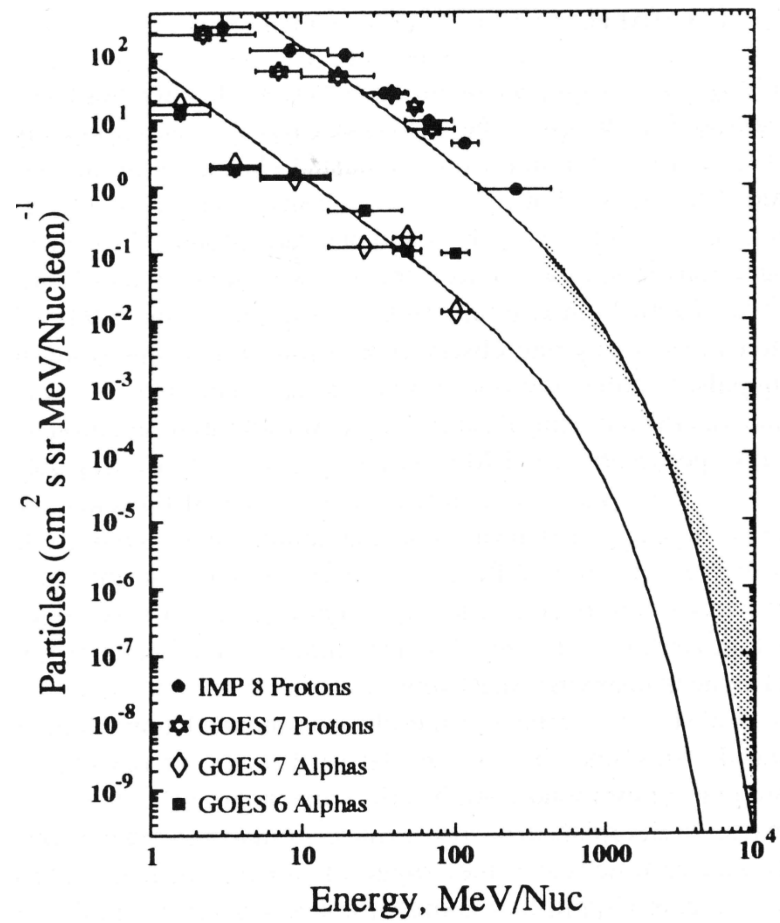

The Sun

Shocks in the heliosphere: each is an energetic-particle source.

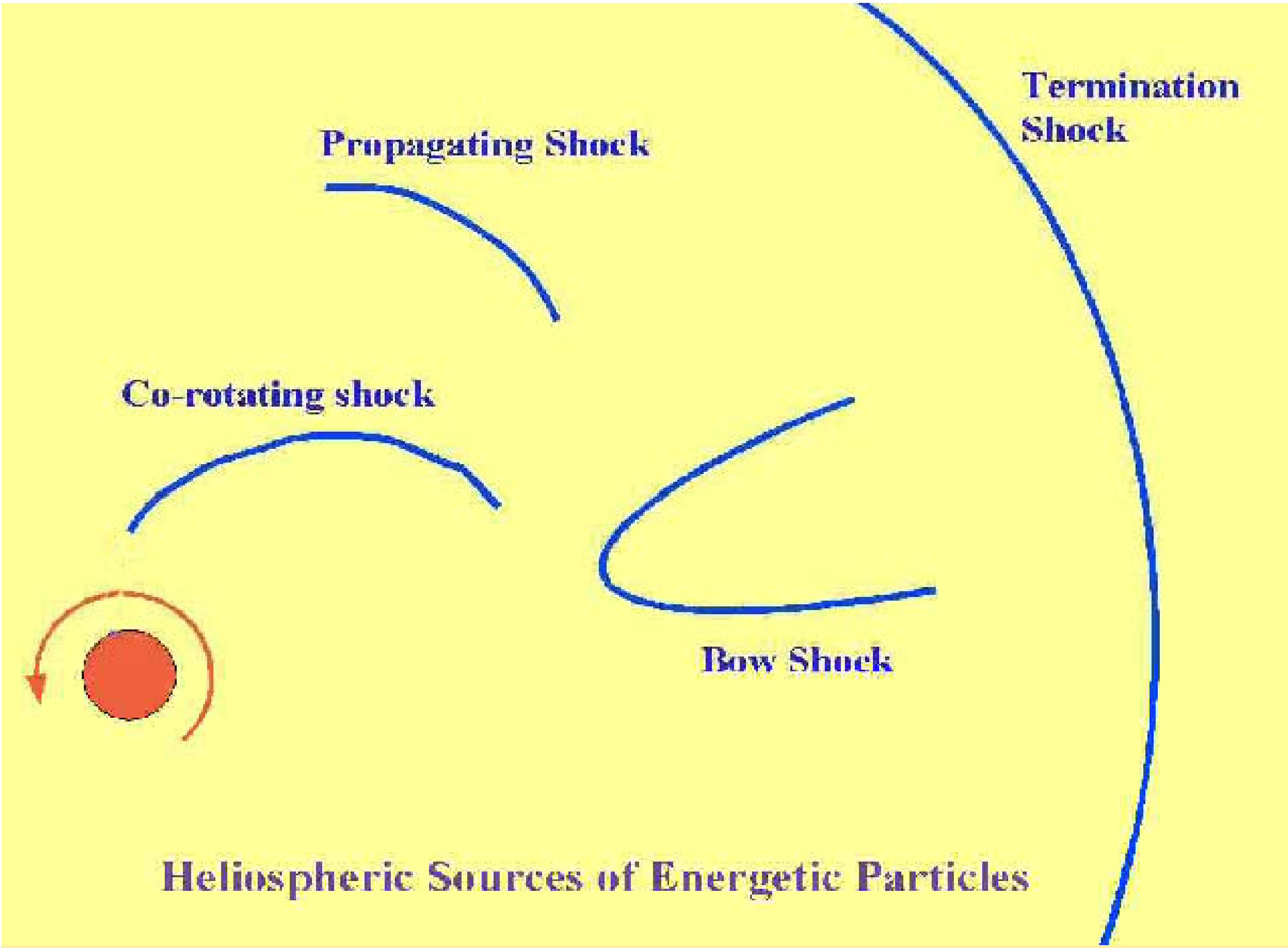

The Parker Equation – first order in w/U

$$\frac{\partial f}{\partial t} = \frac{\partial}{\partial x_i}\left[\kappa_{ij}^{(S)}\frac{\partial f}{\partial x_j}\right]$$ ⇒ **Diffusion**

$$-\mathbf{U} \cdot \nabla f$$ ⇒ **Convection w. plasma**

$$-\mathbf{V_d} \cdot \nabla f$$ ⇒ **Grad & Curvature Drift**

$$+\frac{1}{3}\nabla \cdot \mathbf{U}\left[\frac{\partial f}{\partial \ell np}\right]$$ ⇒ **Energy change**

$$+Q$$ ⇒ **Source**

Where the drift velocity due to the large scale curvature and gradient of the average magnetic field is:

$$\mathbf{V_d} = \frac{pcw}{3q}\nabla \times \left[\frac{\mathbf{B}}{B^2}\right]$$

This is well-tested and established. Not useful at low particle speeds w ~ U. Can be applied to shocks.

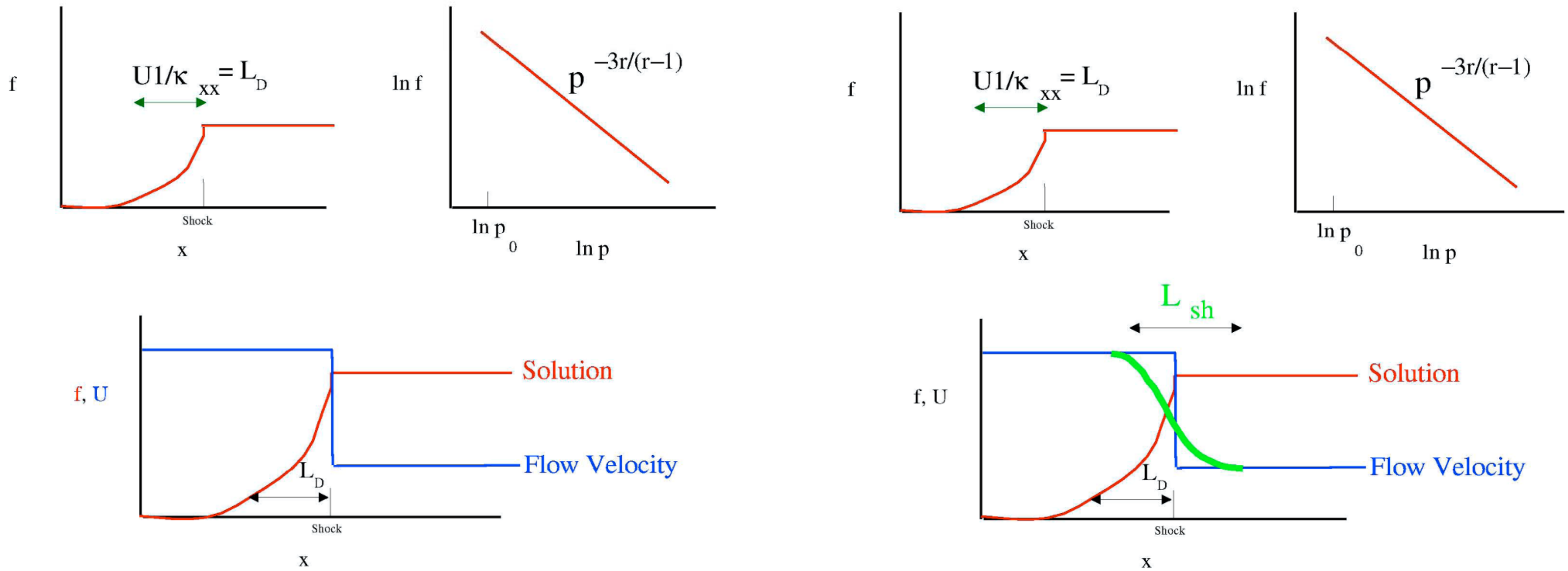

Illustration of the time-asymptotic solution to Parker's equation for a one-dimensional shock.

The spectrum is a power law in momentum with index depending *only* on the shock ratio r.

This predicted behavior is observed at shocks. This led to the well-established paradigm of diffusive shock acceleration. It explained a lot, including the universal energy spectrum.

Kennel, etal,

Unfortunately, this classic observation is not easy to repeat.

Apparently even Kennel et al were forced to look at many shocks before finding the one illustrated.

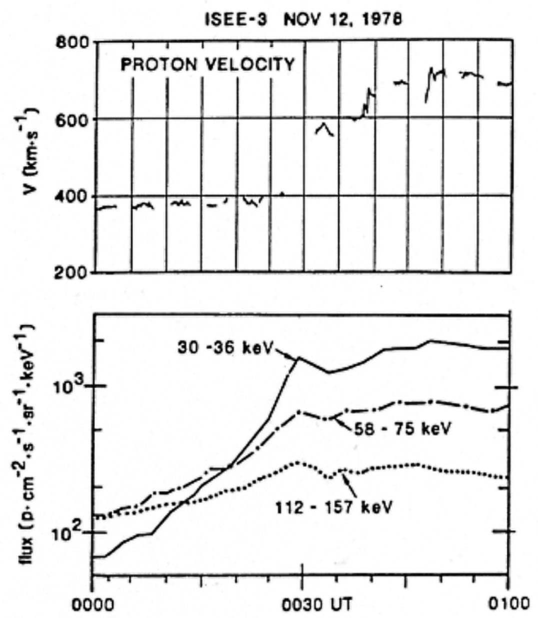

Fig. 1. Solar wind flow speed and energetic protons. The top panel shows the solar wind speed measured by the ISEE-3 solar wind plasma instrument [*Bame et al.*, 1978] and the bottom panel shows the differential fluxes of 30–36 keV, 58–75 keV, and 112–157 keV protons measured by the ISEE-3 nuclear and ionic charge distribution Experiment [*Hovestadt et al.*, 1978]. The period 0000–0100 UT on November 12, 1978, includes the passage of the interplanetary shock over ISEE-3 at 0028:16 UT. The solar wind proton bulk velocity increased slightly, from 380 km s^{-1} to 400 s^{-1}, upstream of the shock and increased to 571 km s^{-1} at the first downstream measurement. The energetic proton fluxes increased roughly exponentially ahead of the shock, with a scale length that increased with increasing energy. The fluxes maximized at the shock, and remained approximately constant downstream of the shock.

But, often the energy spectrum at a given position does not agree with theory, and the accelerated particles were often not observed to peak at the shock crossing .

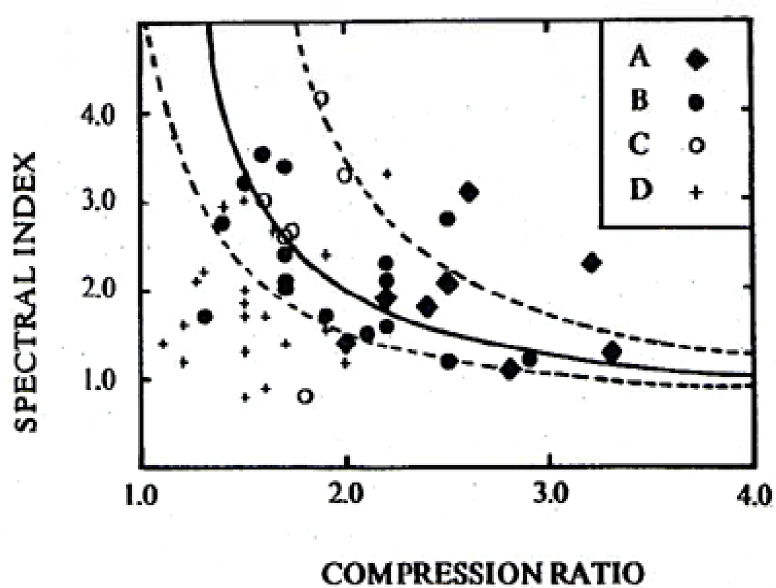

Fig. 12. Spectral index γ plotted as a function of the hydrodynamic shock strength H. The index was derived for the spectrum constructed from the average flux during 10 min immediately after the shock passage. The solid curve indicates the theoretical relation $\gamma = (H+2)(2H-2)^{-1}$. Points within the dashed lines are considered to follow the relation, because of the uncertainty of 25% in H. The events from the different classes are distinguished by different symbols.

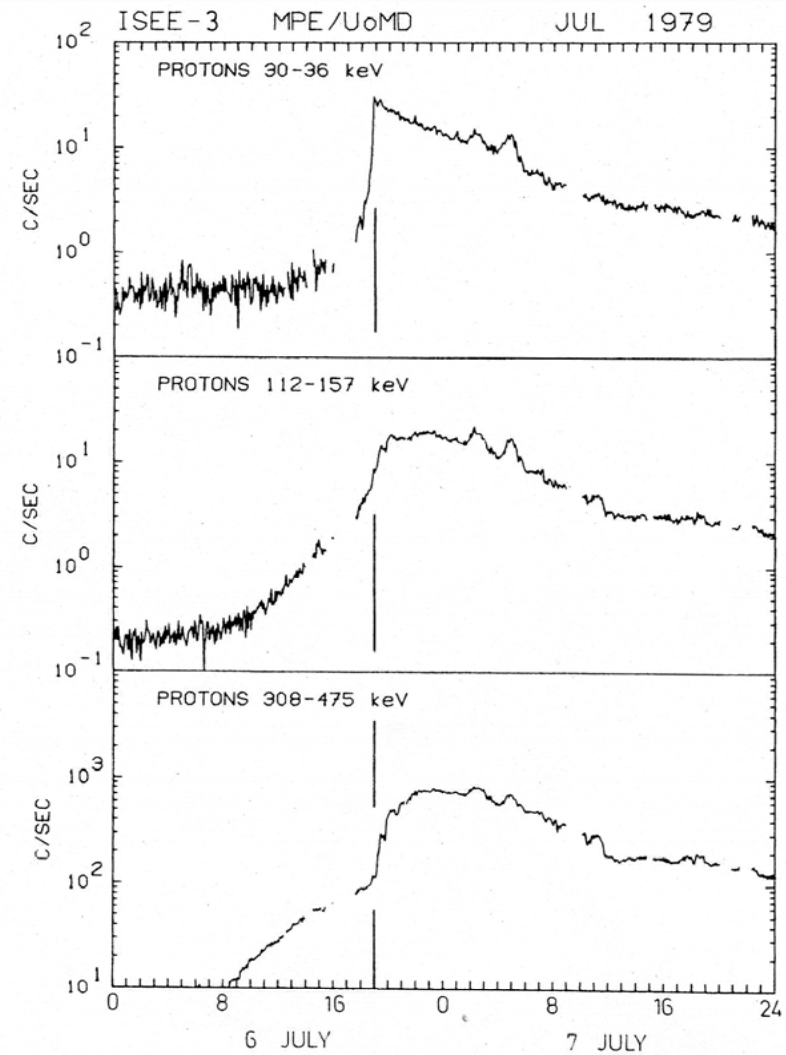

Fig. 10. Intensity-time profiles of low energy protons in three different energy intervals during the July 6–7, 1979, interplanetary shock event. Solid line shows the time of the shock passage.

V

- Hence the nice picture of shock acceleration was <u>too</u> simple.

- It did not agree with many, if not most, observations of energetic particles at propagating shocks.

- A probable interpretation of these various observations is that they are related to the upstream turbulence.

- The propagation of the shock waves through the ubiquitous large-scale turbulence in the plasmas causes significant, changes to the shock which are essentially unpredictable.

- The properties of individual shock waves vary in important ways both along the shock face and as a function of time along the shock.

- Different spacecraft crossing the same shock at different points will generally see quite different phenomena.

- These phenomena are best studied statistically, using data from multiple shock crossings, by multiple spacecraft.

A cartoon illustrating the interaction of a shock with pre-existing turbulence.

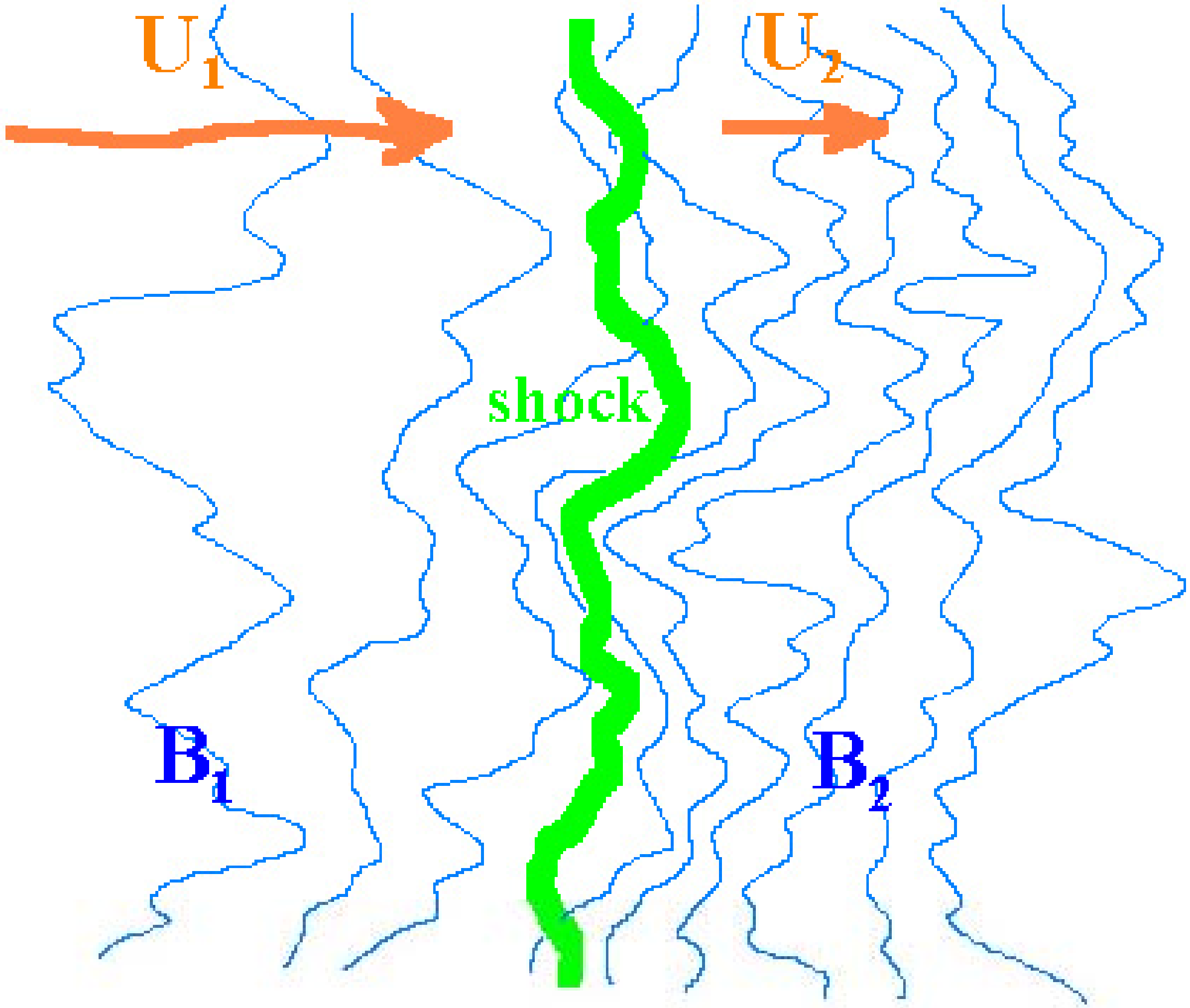

“rippled” interplanetary disturbances (STEREO/HI2 difference images)

May, 27 2008

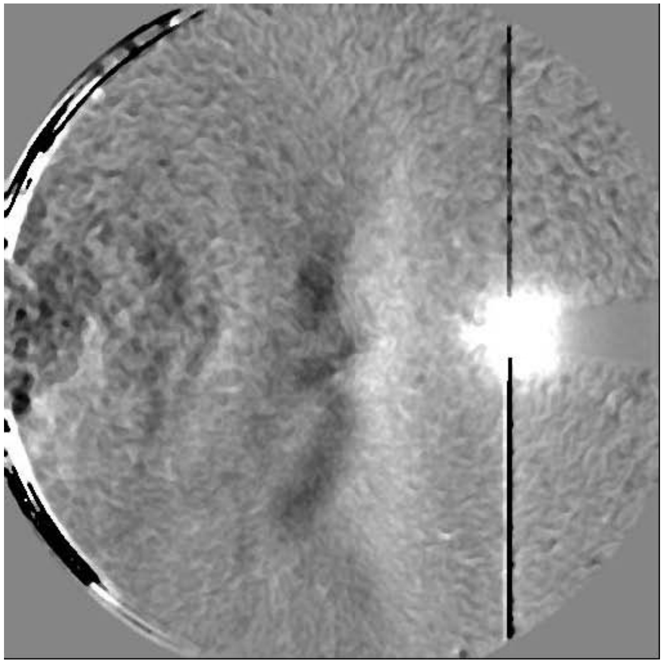

Dec 16 2007

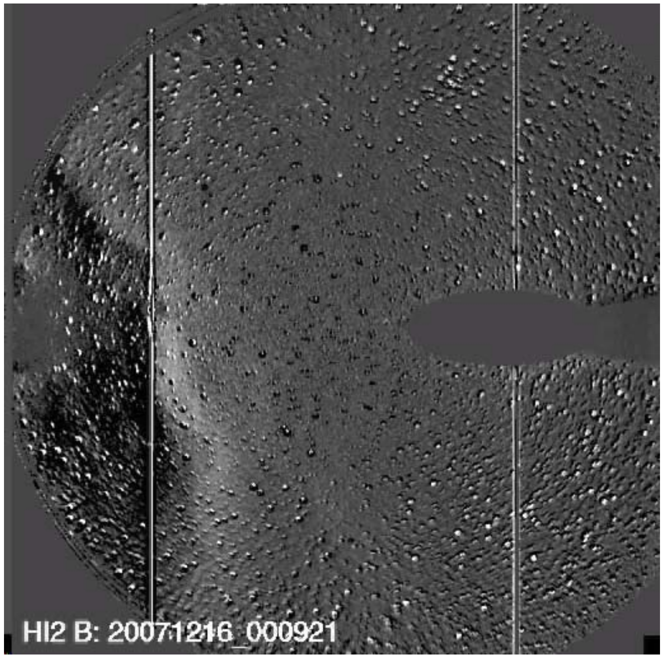

We at Arizona have suggested that many of the difficulties can be understood in terms of pre-existing, large-scale turbulence interacting with a shock.

Interplanetary shocks locally seem to be analogous to this tidal bore.

Hybrid Simulations of a perpendicular shock moving through a turbulent plasma show suggestive behavior. (Neugebauer and Giacalone, 2005)

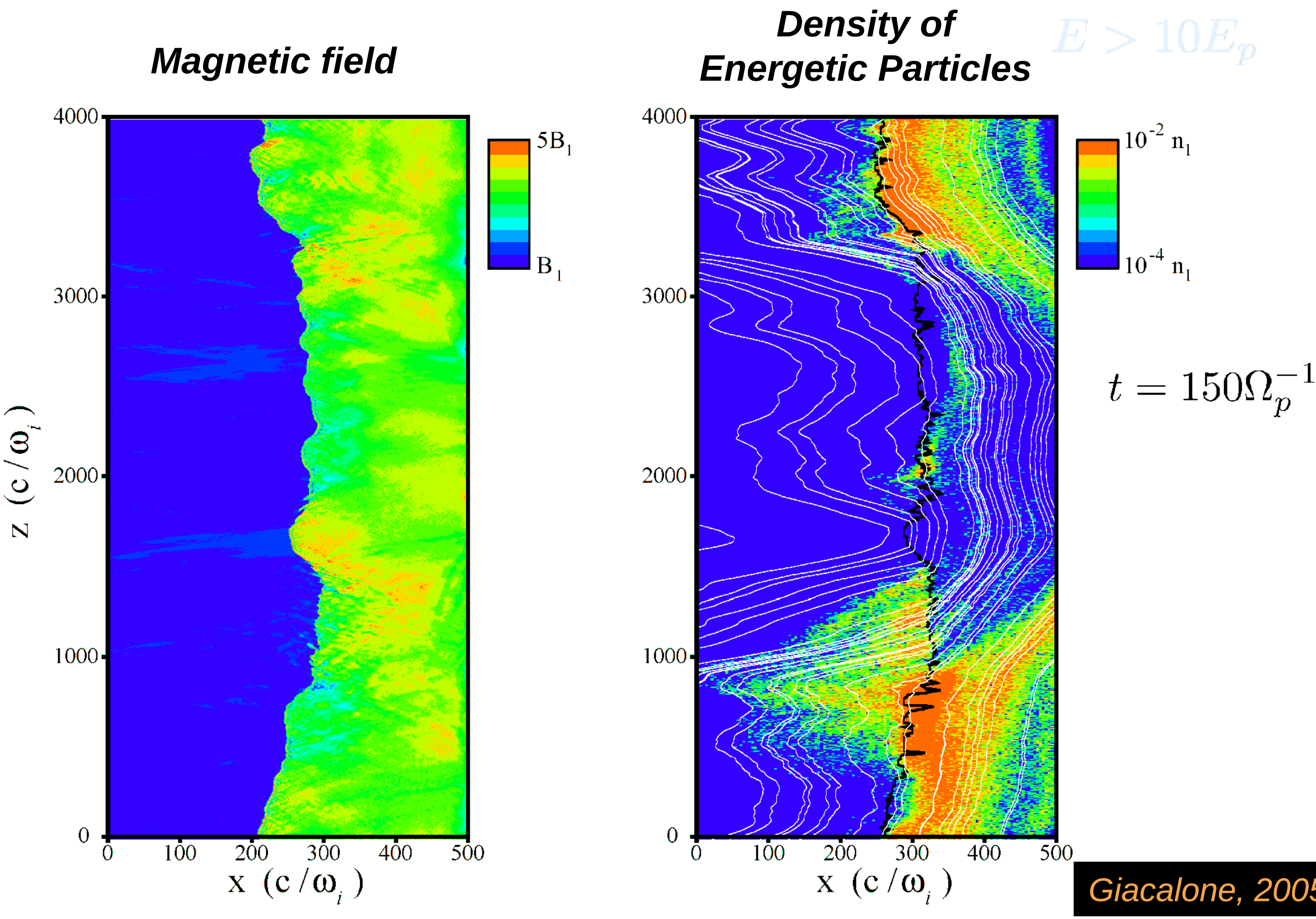

Giacalone, 2005

Multiple-Spacecraft Observations Allow Determination of Shock Shape and Normals

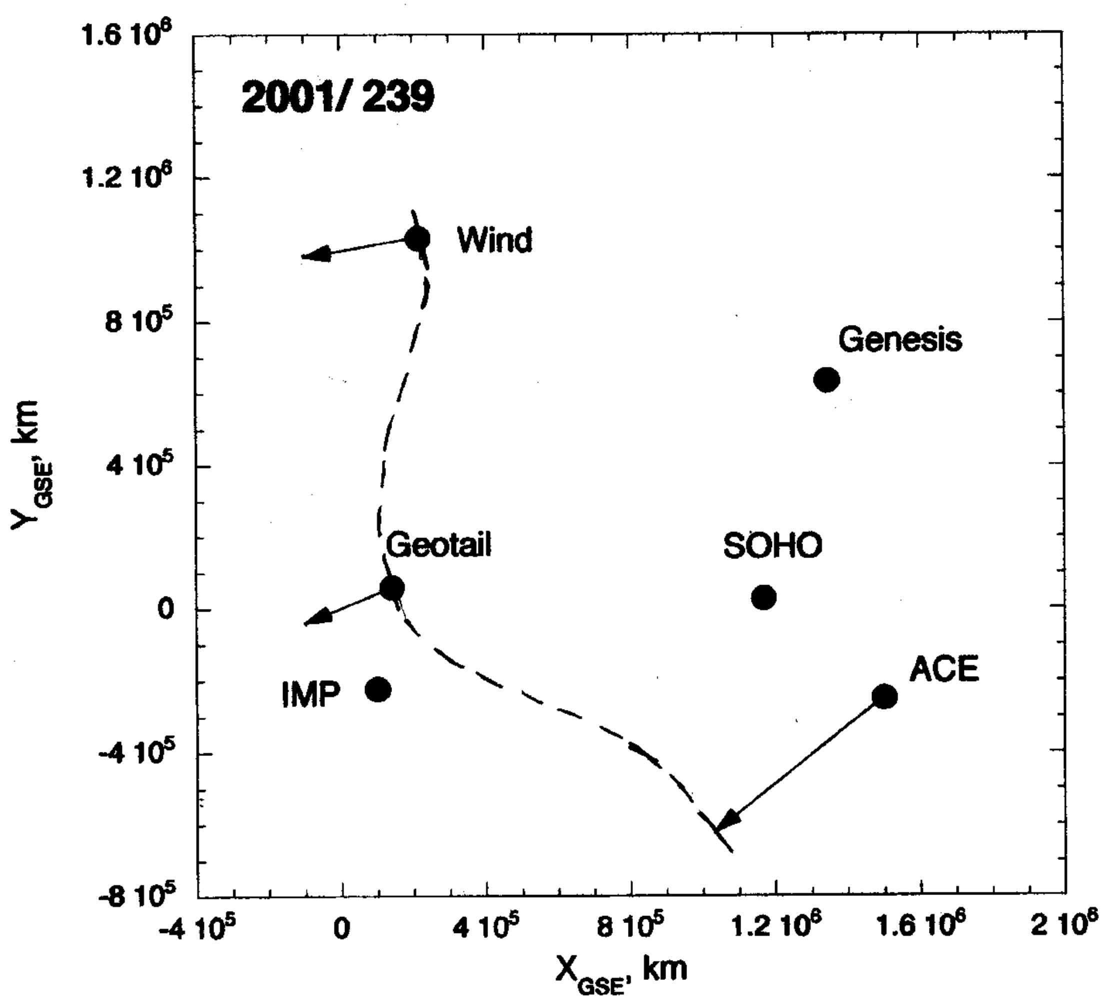

Wind/Geotail saw this shock nearly simultaneously

Obs. at ACE is used to predict shock location at the time of Wind/Geotail observation

Distribution of shock radii of curvature

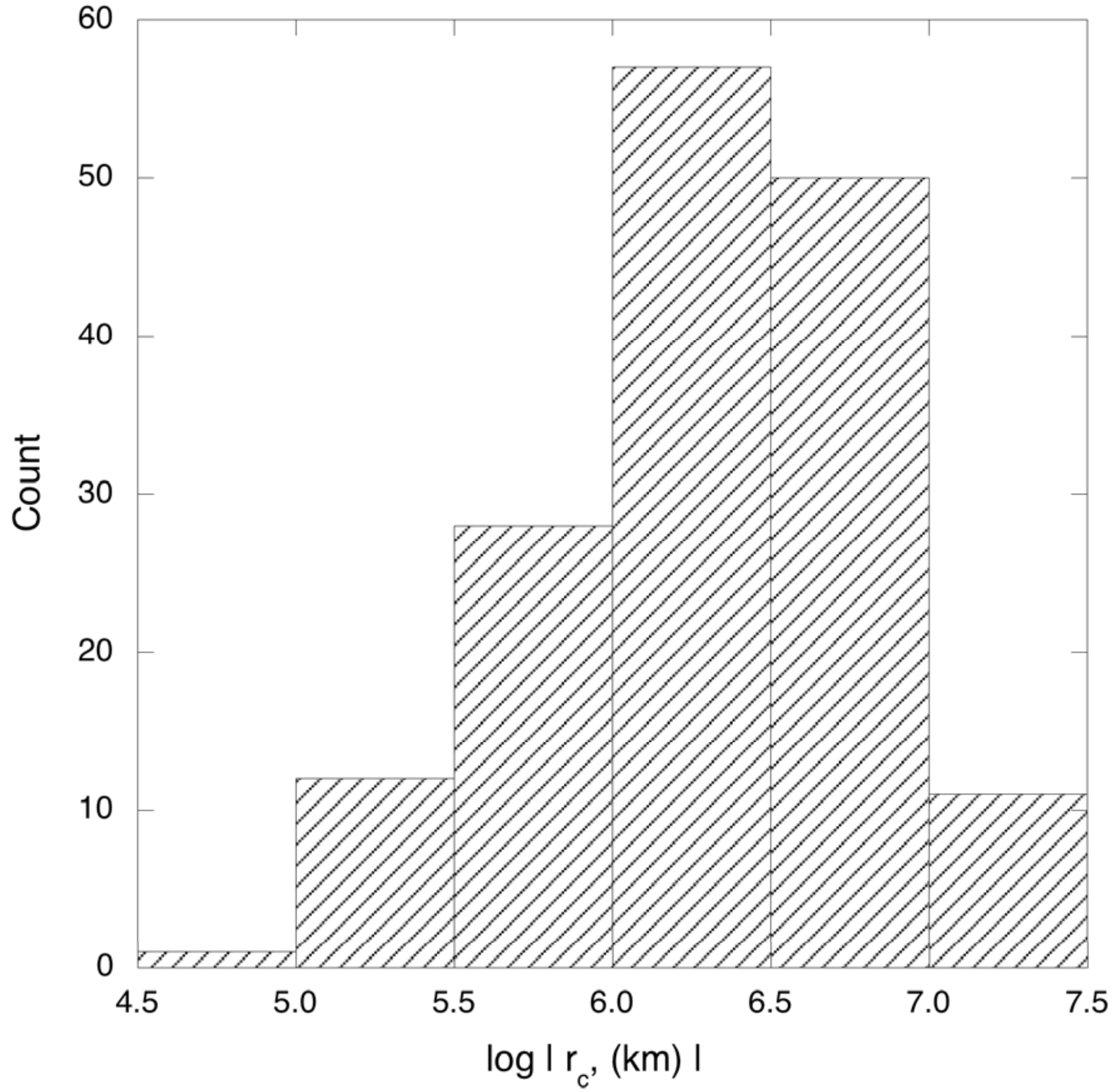

Energetic particles also differ at different locations on the same shock.

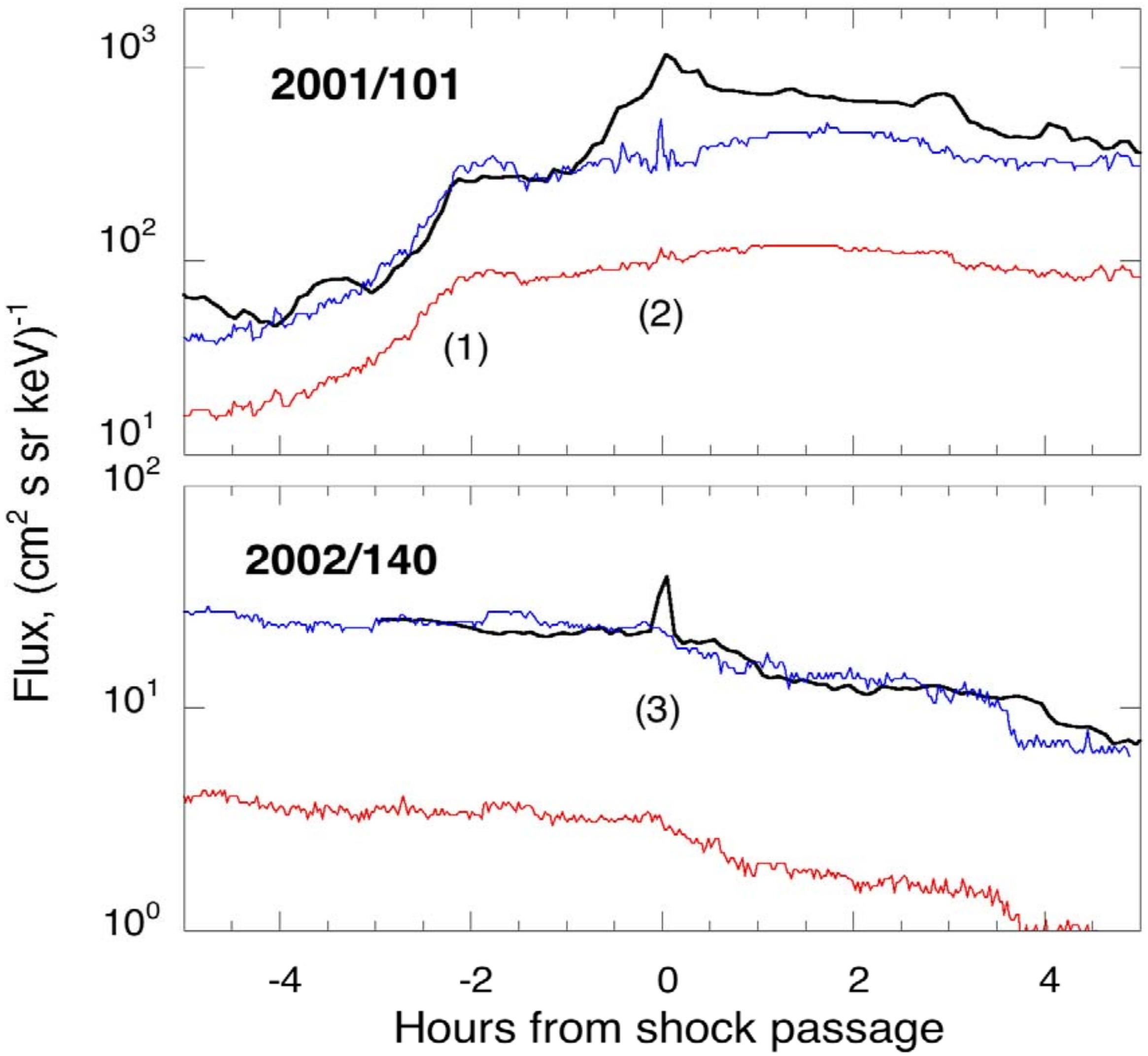

The coherence scale of the energetic-particle variations is about 1-2 million km.

This is the coherence scale of interplanetary turbulence.

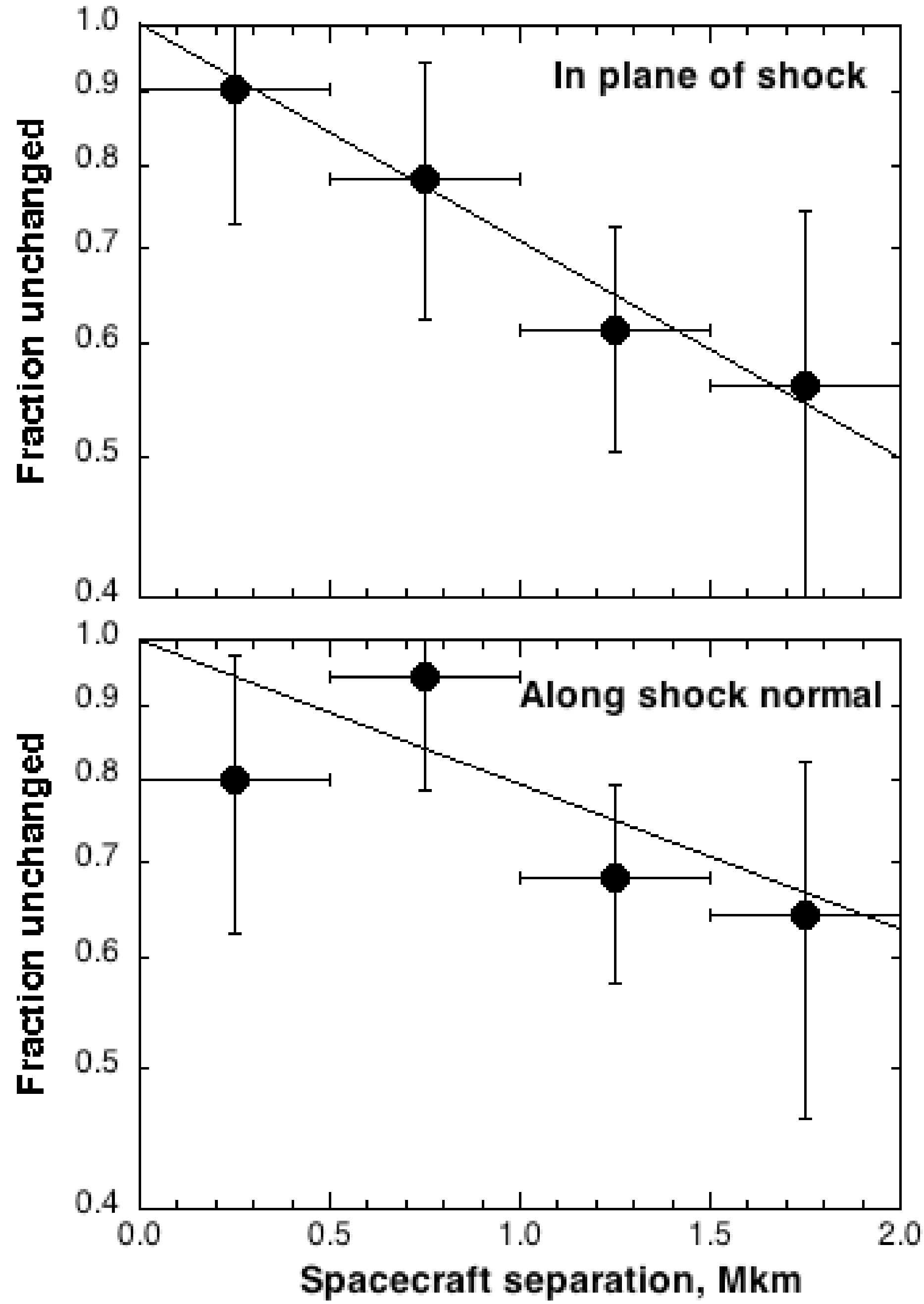

Conclusions from these considerations and multi-spacecraft observations:

- Shock ripple radius of curvature = 2-3 Mkm.
- Persistence of EP features for L~3 Mkm
- Comparable to the correlation length of interplanetary magnetic field $\sim L_c \sim$ 2 Mkm.
- We suggest that these are caused by pre-existing interplanetary turbulenc.

The heliospheric termination shock shows similar behavior.

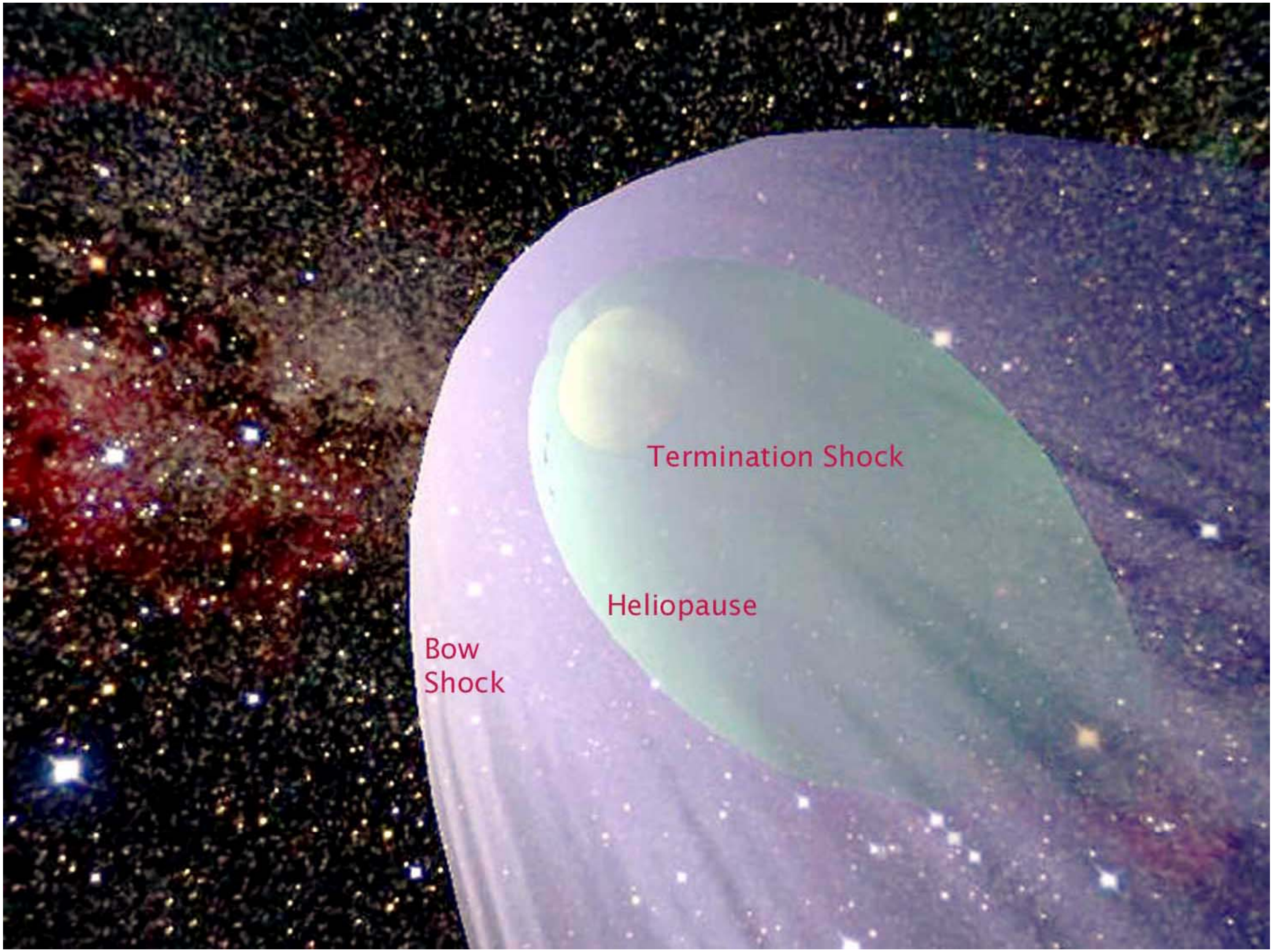

An instructive analog may be seen in a kitchen sink.

J. R. JOKIPII

A more-accurate analog model was created by Prof. Hsieh
Of the University physics department.

The Voyager 2 Termination Shock Crossing Provided Strong Evidence for such Turbulence

- The functioning plasma detector helped to provide richer data set than from V1.
- Also, the crossing was at a much slower shock speed.

The multiple crossings in a few days argued for a turbulent shock

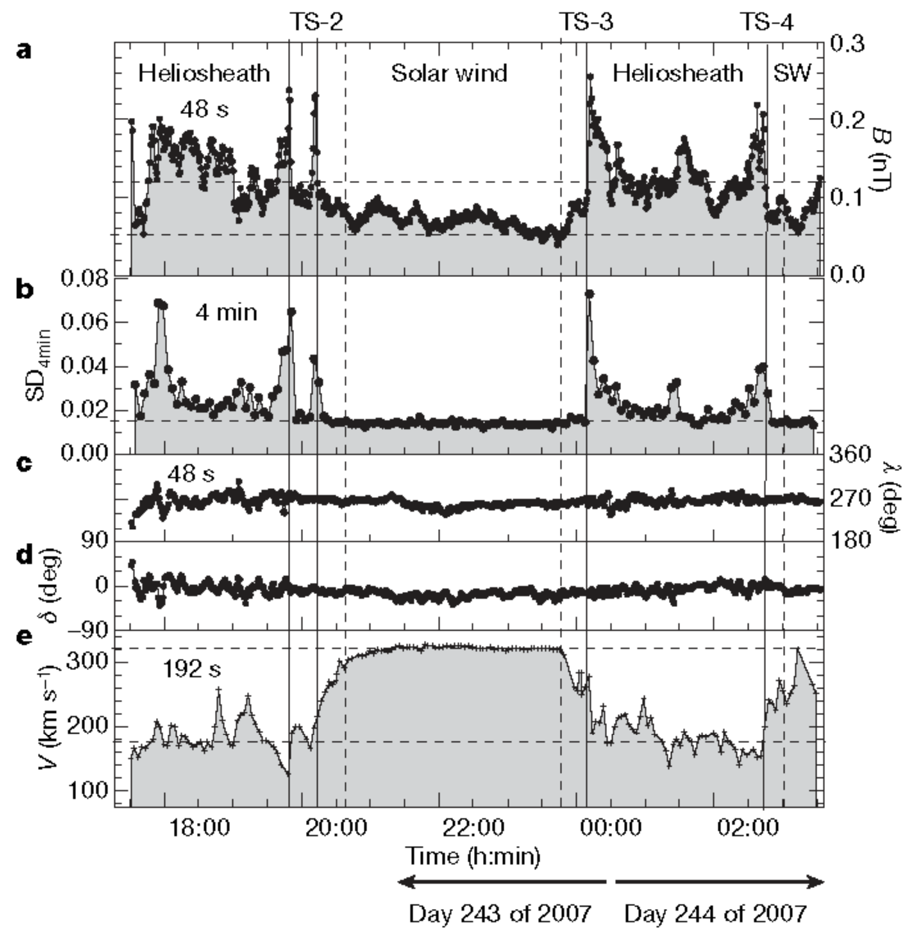

The multiple crossings in a few days argued for a turbulent shock.

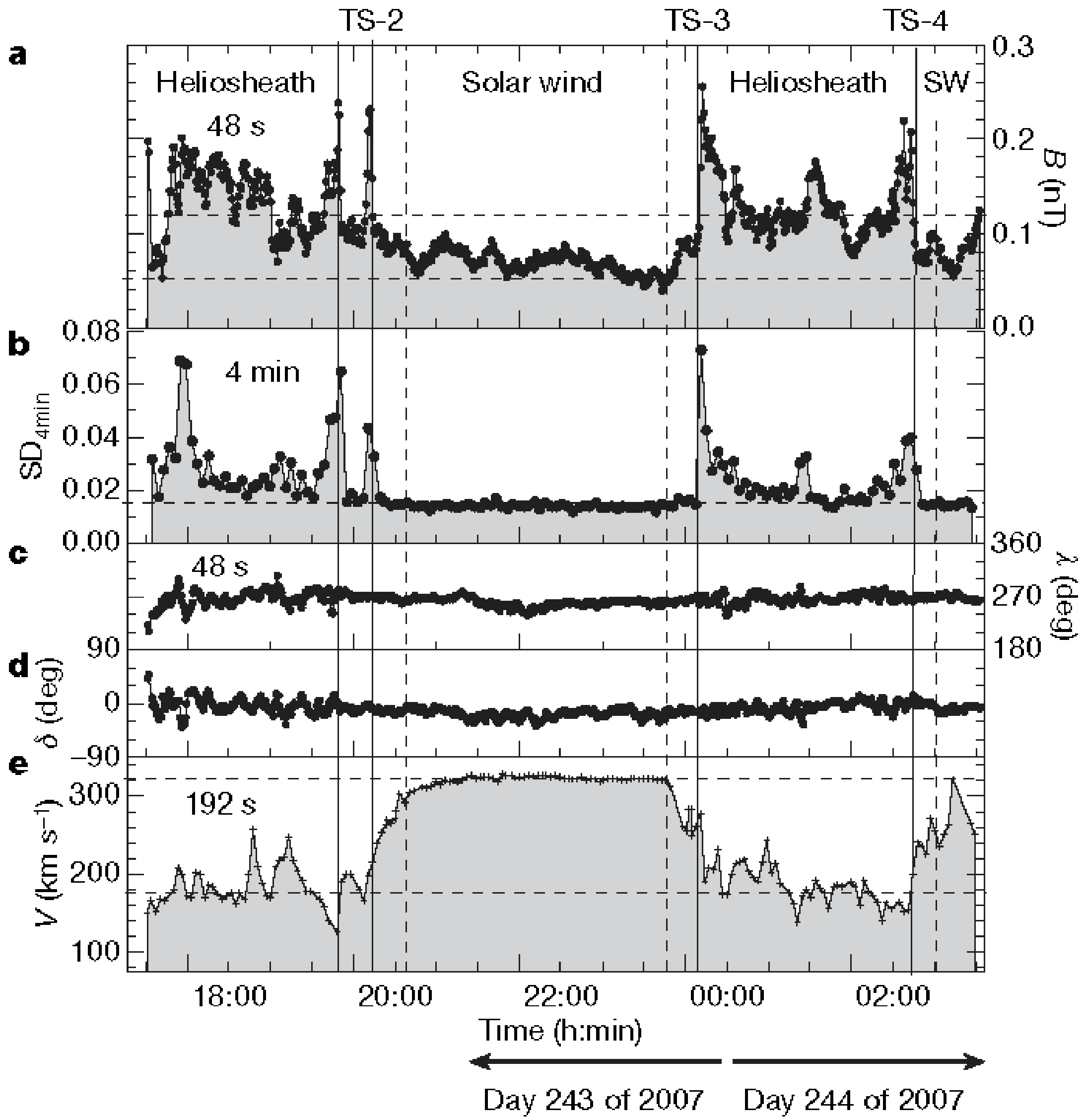

Acceleration of anomalous cosmic rays (ACR) probably occurs at the heliospheric termination shock. They serve as valuable remote probes.

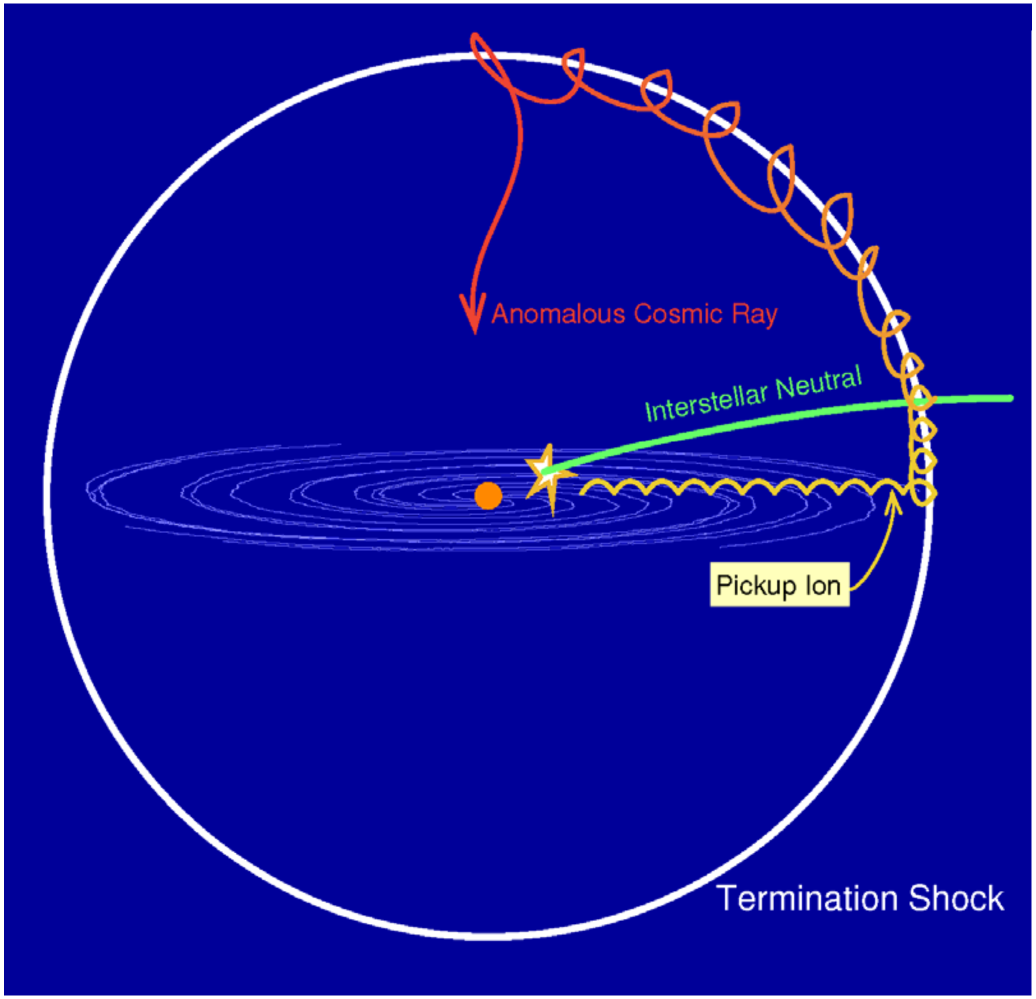

ACR model spectra computed using Parker's equation, showing the 'unfolding' of the energy spectrum with increasing radius inside the shock and decreasing intensity beyond.

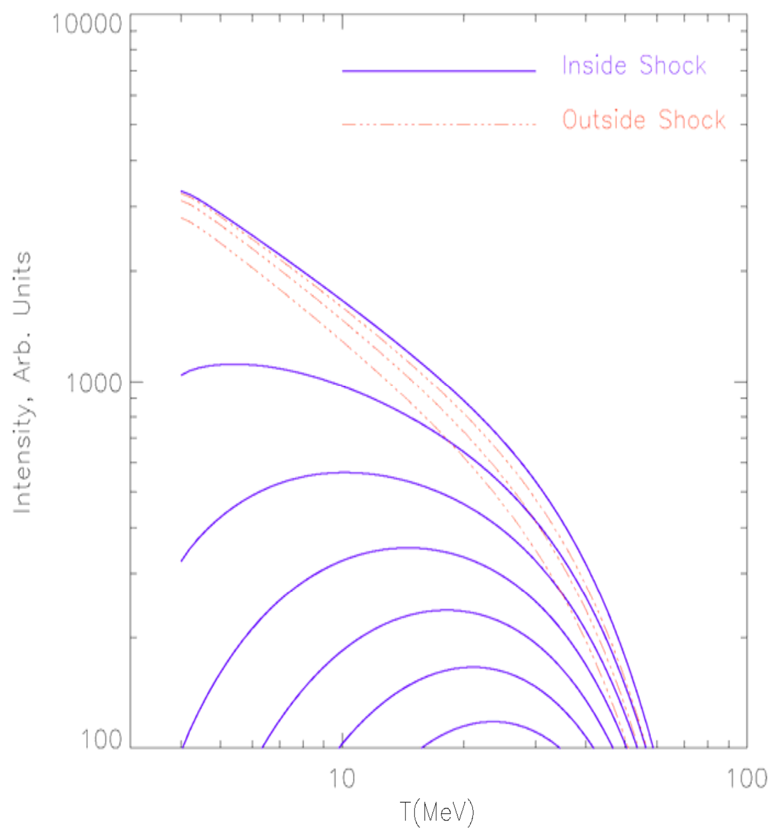

Voyager 1 observations of Cummings, Stone and Webber, 1996

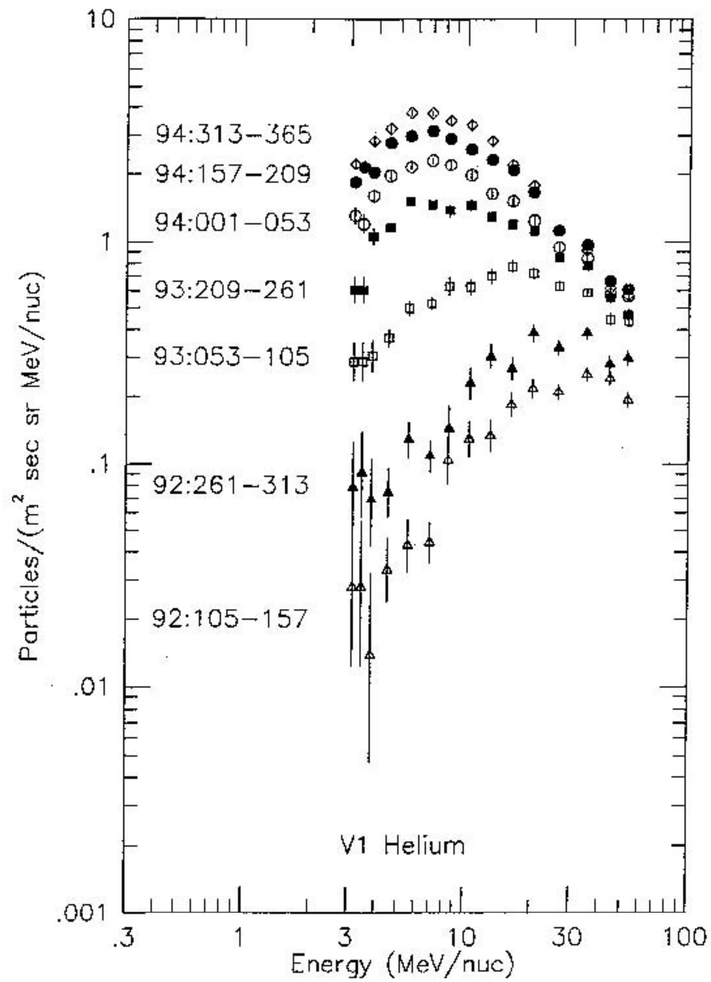

Figure 3. Energy spectrum of helium measured at V1 for seven time periods.

The radial dependence obtained from solving Parkers equation for a termination shock.

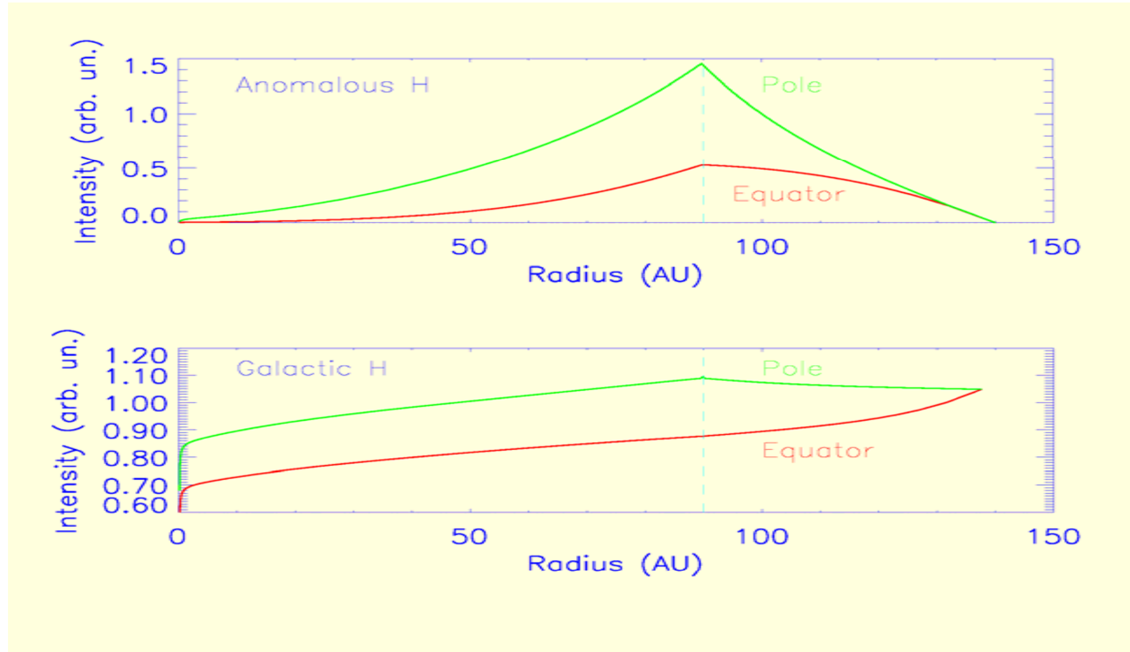

What was actually observed at the termination shock.

We attribute this discrepancy to turbulence hitting the shock..

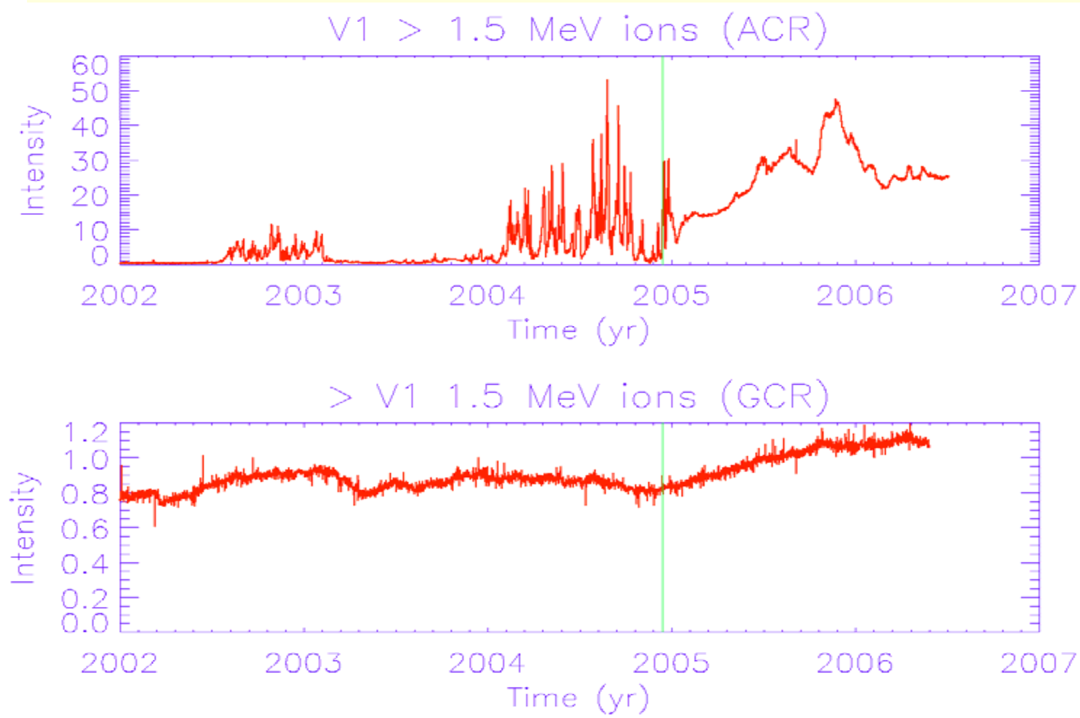

This image from Berezhko and Volk, 2005 is suggestive:

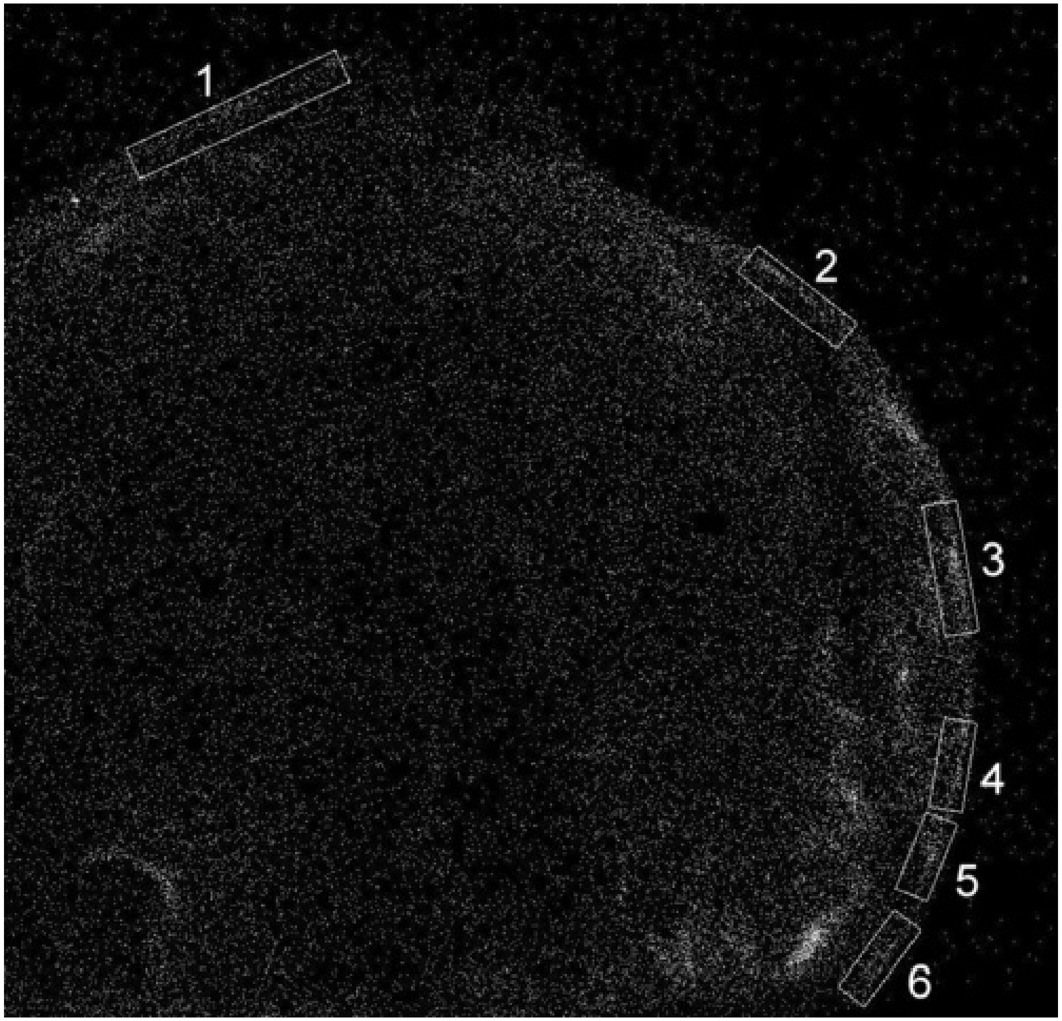

Giacalone & Jokipii, 2007 considered the effect of density turbulence on a strong shock.

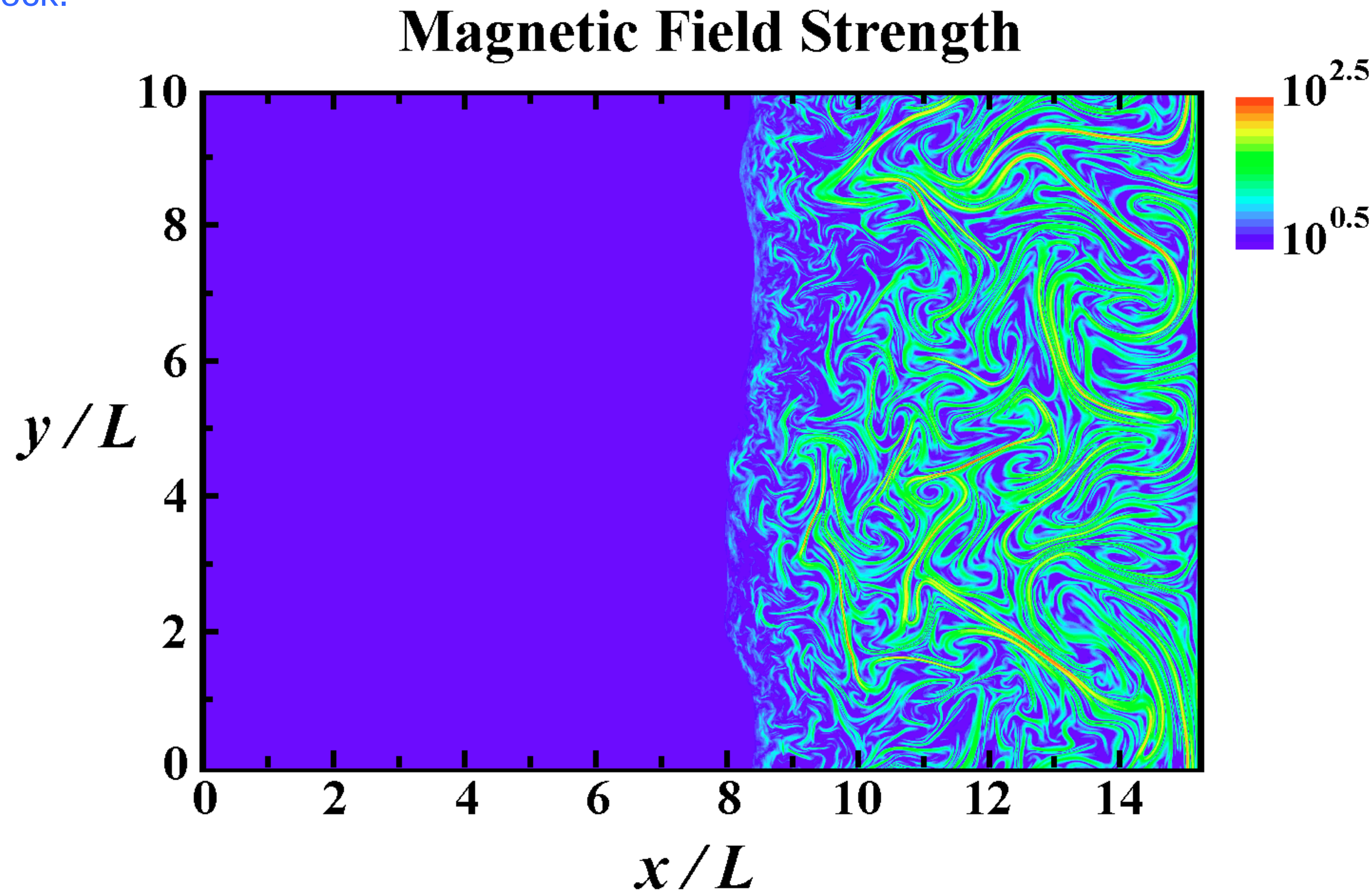

This is similar to what Inoue discussed yesterday. But we used parameters representative of the general ISM

Mean Downstream Field Strength

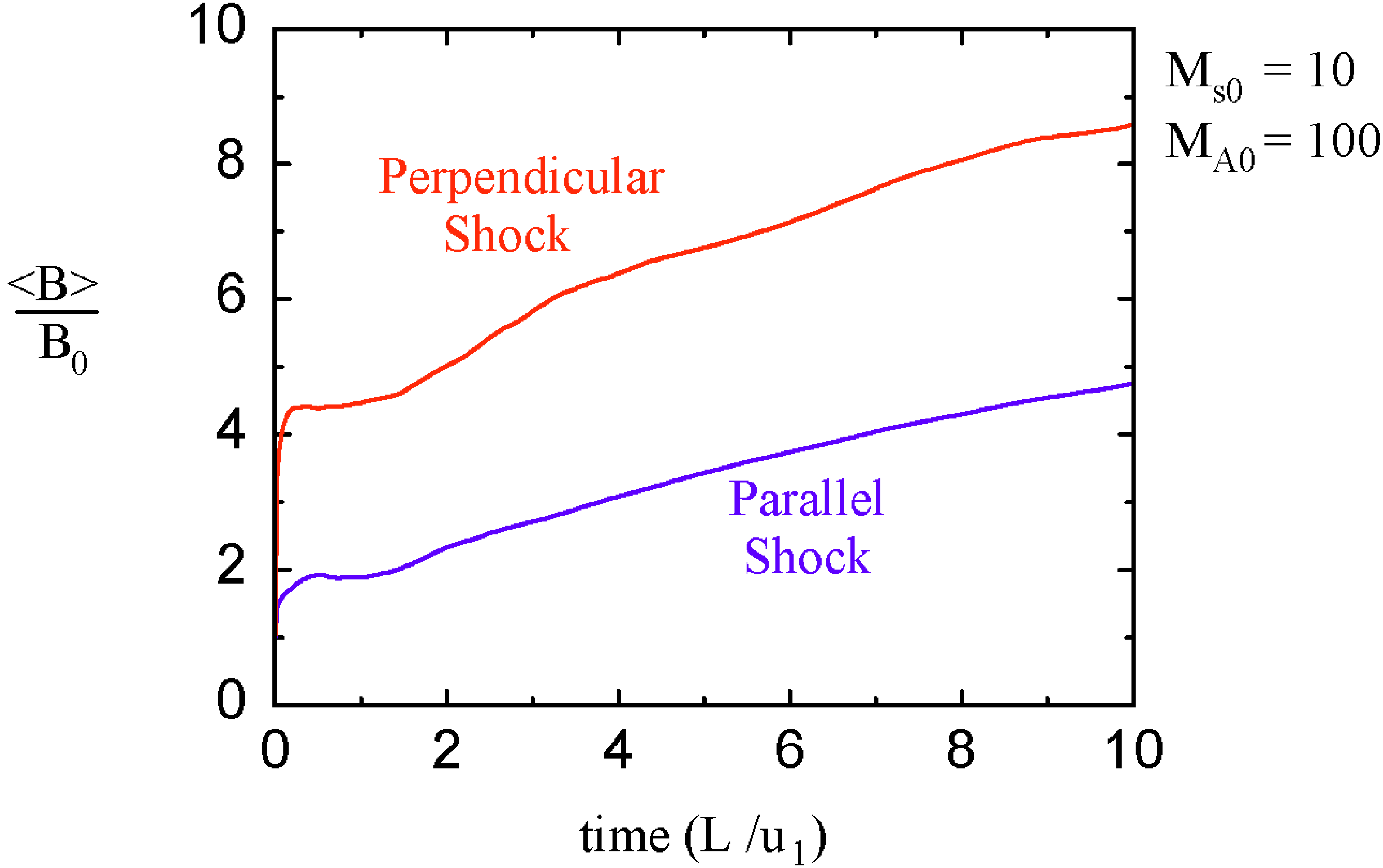

Interpretation:

The enhanced *B* downstream of a shock moving through density turbulence (without cosmic-ray excited waves!) is due primarily to the **induced downstream vorticity** and is ***quite robust***.

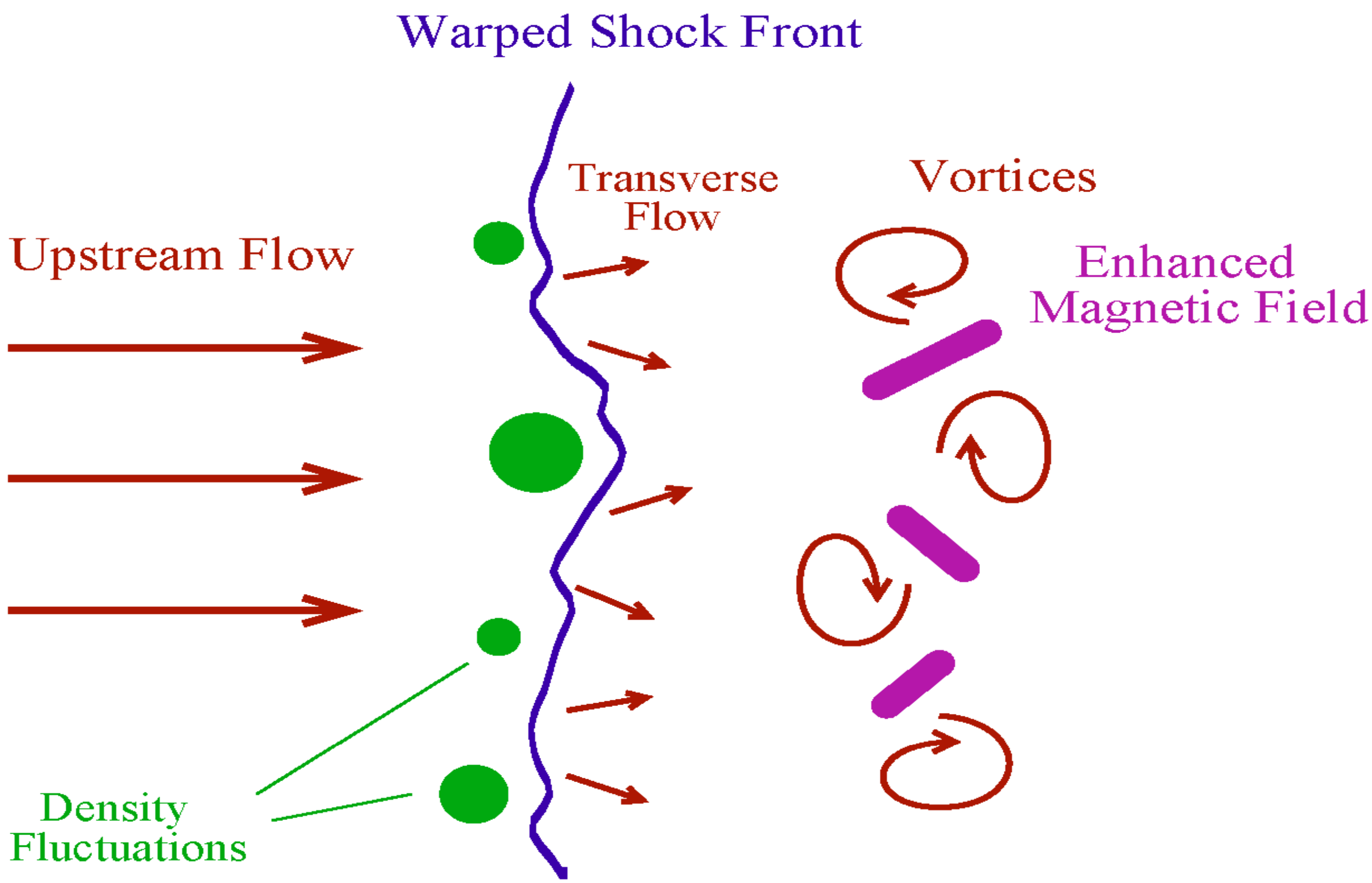

Conclusions

- Collisonless shock waves are observed in the heliosphere from the Sun to the termination shock of the solar wind.
- They produce many different populations of energetic particles.
- Recent analyses suggest that many of the anomalies seen are the result of the shocks interacting with pre-existing,upstream turbulence.
- Application of these ideas to a strong blast wave suggests that upstream density turbulence may be responsible for the strong magnetic fields observed in supernova remnants – as an alternative to upstream instabilities.